

EXPERIMENTAL EFFECTS OF SCALING ON THE PERFORMANCE OF ION
ROCKETS EMPLOYING ELECTRON-BOMBARDMENT ION SOURCES

By Paul D. Reader
Lewis Research Center
National Aeronautics and Space Administration
Cleveland, Ohio

Presented at the National IAS-ARS
Joint Meeting, Ambassador Hotel,
Los Angeles, California, June 13-16,
1961.

61-87-1781

Publishing rights reserved by American
Rocket Society. Abstracts may be
published without permission if credit
is given to the author and to ARS.

FACILITY FORM 802	N65-87115	
	(ACCESSION NUMBER)	(THRU)
	30	None
	(PAGES)	(CODE)
	TMX-56487	
	(NASA CR OR TMX OR AD NUMBER)	(CATEGORY)

EXPERIMENTAL EFFECTS OF SCALING ON THE PERFORMANCE
OF ION ROCKETS EMPLOYING ELECTRON-BOMBARDMENT
ION SOURCES

By Paul D. Reader

Lewis Research Center
National Aeronautics and Space Administration
Cleveland, Ohio

ABSTRACT

Previous investigations have shown that the electron-bombardment ion rocket holds considerable promise as a mechanically simple, reliable, and efficient space propulsion device. A scaling program was undertaken to establish the relations between performance parameters and the size of the electron-bombardment ion source. The experimental results of this investigation are the subject of this paper.

Three ion beam sources were fabricated and tested in one of the 5-ft-diameter, 16-ft long vacuum tanks at the NASA Lewis Research Center. The first of these, a 10-cm-diameter beam source, has achieved power efficiencies over 80 percent at a specific impulse of 8300 sec. It has been operated continuously for 10 hr at thrust levels above 10 millipounds. Beam currents of 1/2 amp have been attained yielding thrust values of up to 20 millipounds at 8300 sec.

Two geometrically similar sources, a 5- and a 20-cm-diameter beam source, were scaled from the 10-cm-diameter source to allow a performance comparison to be made. The same grid spacing was used for all accelerator systems so that constant current per unit area would be expected.

The three ion sources are compared for ion chamber characteristics and overall power efficiency. The effects of size on operating limits are also discussed. Mercury was used as the propellant in this investigation.

INTRODUCTION

Previous investigations have shown that the electron-bombardment ion rocket holds considerable promise as a mechanically simple, reliable, and efficient space propulsion device.^{1,2} A scaling program was undertaken to establish the relations between performance parameters and the size of ion rockets employing electron-bombardment ion sources.

The maximum size of an individual thrust unit of an electron-bombardment ion engine is dependent on both ion chamber and accelerator scaling relations. The ion chamber scaling problem resolves to the question of whether or not the chamber will operate as effectively in sizes other than the 10-cm size first investigated. This effect of size on performance is the subject of this report.

The accelerator scaling problems encountered thus far result from manufacturing tolerances, alignment, thermal expansion, and warping and are felt to be more in the nature of development rather than research problems.

Three geometrically similar ion beam sources were fabricated and tested in one of the 5-ft-diameter, 16-ft long vacuum tanks at the NASA Lewis Research Center. Use of a 5-, a 10-, and a 20-cm-diameter beam source allowed a performance comparison to be made over a 4:1 diameter range. The same grid spacing was used for all accelerator systems so that constant current per unit area would be expected. The magnetic field configurations were geometrically similar. The three ion sources are compared for both ion chamber performance and overall engine power efficiency. Ion chamber losses are

compared in terms of electron volts per beam ion. The effects of size on the operating limits are also discussed. Mercury was used as the propellant in this investigation.

OPERATION

The 20-cm-diameter engine is shown in Fig. 1(a). A cutaway sketch of the engine type tested is also shown in Fig. 1(b). The propellant gas enters through the distributor. This gas is ionized by high-velocity electrons (20 to 100 v), which are emitted by a hot filament. The screen, the distributor, and the negative end of the filament are operated at the same potential. Thus, an electron emitted from the filament should not go to either end of the ion chamber. A magnetic field approximately parallel to the axis prevents the high-velocity electrons from reaching the wall without first colliding with particles in the ion chamber. Some of the ions that are formed pass through the screen at the downstream end of the ion chamber and are accelerated to become the beam.

Several parameters must be held constant to afford a common ground for comparison of different size ion sources. During this investigation the comparative data were taken with the particle exhaust velocity, the ion chamber density, and the propellant utilization efficiency held constant. To keep the electric field gradient effects on the plasma boundary at the screen as constant as possible, the same gross accelerating potential (6000 v) and aperture size ($3/16$ -in. holes) were used for the accelerator grids on all three sources during most of the investigation. Hence, constant current per unit area through the accelerator system would be expected. Most ion chamber performance comparisons were also made at a constant net accelerating potential, thus maintaining a constant particle exhaust velocity corresponding to

a specific impulse of 7000 sec. Some data were also obtained over a range of specific impulse to show the effect of this parameter on performance. The accel-decel ratio was maintained at approximately 4:1 during the entire investigation.

The beam currents during the investigation were $1/2$ amp for the 20-cm-diameter source, $1/8$ amp for the 10-cm-source, and $1/32$ -amp for the 5-cm-diameter source. The propellant utilization efficiency was maintained at 80 percent throughout the investigation by scaling the propellant flow.

The magnetic field shapes were also similar for each of the three sources. The field lines diverged in the downstream direction to give a value of field strength at the screen which was 60 percent of that at the distributor. All field strengths reported in the data are those at the screen.

DISCUSSION AND RESULTS

A proper measure of ion chamber efficiency is the energy dissipated in the ion chamber discharge per beam ion. Fig. 2(a) shows the ion chamber performance of the 20- and 10-cm-diameter sources at a magnetic field strength of 17 gauss. The ion chamber losses in electron-volts per beam ion are plotted against the ion chamber potential difference, the potential between the emitter and anode. The performance of the 20-cm source is better than the 10-cm source, the difference becoming more pronounced at higher ion chamber potential differences. Fig. 2(b) shows the comparison between the chamber performance of the 10- and 5-cm-diameter sources at a field strength of 32 gauss. Again the larger source has superior ion chamber performance. This result is to be expected since the cyclotron radius of the high-velocity ionizing electrons (20 to 100 ev) was maintained constant for each field strength, which would have the effect of reducing electron containment as

the source diameter was reduced. The engines could not all be compared at the same field strength because of operational limits for the field windings and power supplies.

Fig. 2(c) shows the ion chamber losses of the three engines compared at scaled magnetic field strengths. The scaling was accomplished by holding the product of the magnetic field strength and ion source diameter constant. This would produce a constant ratio of electron cyclotron radius to anode radius in each of the sources.

The experimental data are in much closer agreement under these conditions. The 10-cm-diameter source has the best performance followed closely by the 20-cm source. The 5-cm source has by far the poorest ion chamber performance. This low performance is felt to be due to the radial potential variation in the small chamber.

The expression for the radial potential variation in the chamber is¹:

$$\Delta V_{\text{rad}} = \frac{10^{11} J_- \bar{V}_-^{1/2}}{2\pi L_c^2 n_-^2 \sigma_E}$$

where

l ion chamber length

J_- electron current

L_c electron cyclotron radius

n_- electron density

\bar{V}_- electron thermal potential

σ_E effective cross section

The ion chamber length was made proportional to the diameter, and with a scaled magnetic field the cyclotron radius was also proportional to diameter. Assuming similar operation within the ion chamber, both the electron thermal

potential (plasma temperature) and cross section should be independent of size. The electron current should be proportional to beam current density times the source diameter squared. The electron density should be proportional to the beam current density. Thus the radial potential difference varies as

$$\Delta V_{\text{rad}} \propto \frac{1}{Dj}$$

If the current density is also held constant, the radial potential difference varies only as D^{-1} . With the radial potential difference varying inversely with the diameter of the source it would not be unreasonable to expect that a minimum size might be reached at which the major portion of ion chamber power goes, not into the ionization process, but into ohmic heating of the plasma.

The ratio of emission current to beam current for both the 10- and 20-cm sources when operating at 80-percent propellant utilization was approximately 10:1. The ratio for the 5-cm source at 80-percent utilization was 50:1, thus tending to support the above-mentioned theory.

Fig. 3 shows the effect of magnetic field strength on accelerator impingement current at a specific impulse of 7000 sec. Using mercury as the propellant this impulse corresponds to a net accelerating potential of 4800 v. Accelerator impingement current divided by the beam current is plotted against the magnetic field strength at the screen. The data points are presented to show that at the current density used for these tests, 30 amp/sq m, the ratio of impingement to beam current was nearly constant at 0.006 for most of the magnetic field range investigated.

The impingement on the accelerators of the 20-cm-diameter source was constant until a field strength of approximately 17 gauss was reached. Above 17 gauss it rose rapidly. This rise is most probably due to a local

density-radial potential difference effect in the plasma giving a nonuniform current density distribution at the accelerator system. The phenomenon has been noted in both of the smaller sources at chamber densities and exhaust velocities other than those considered in this investigation. A more complete discussion of this phenomenon, however, is beyond the scope of this paper.

Fig. 4 shows the effect of magnetic field strength on ion chamber efficiency for each source at a constant chamber potential difference of 50 v. Each curve extends from the lowest field strength at which the scaled beam current could be maintained to the point at which either the accelerator impingement increased rapidly or the current carrying capacity of the magnetic field coil was reached. The ion chamber performance levels fall in the same order as those displayed in Fig. 2(c), the 10-cm source reaching the lowest minimum followed closely by the 20-cm-diameter source. The 5-cm-diameter source again has chamber losses approximately 5 times the 10- and 20-cm sources. The losses for each source drop rapidly to a fairly constant value. The most efficient operation is of course attained by operating at the minimum combined ion chamber and field coil losses.

All the preceding data were at a constant accelerating potential difference. The performance was also investigated over a range of specific impulse and, hence, accelerating potential difference. The results are shown in Figs. 5 and 6. The ion chamber potential difference was held at 50 v, the scaled field strengths were used, and the accel-decel ratio was held approximately constant at 4:1. The decreasing ion chamber losses with increasing specific impulse are due to the increasing electric field gradients at the downstream face of the plasma caused by the greater accelerating potential difference. The effects on the 20- and 10-cm sources are very similar. The

5-cm source improves more rapidly than the two larger sources at low specific impulses but tends to level out above 9000 sec. The more rapid increase may be due to the large aperture- to anode-diameter ratio of the small engine. The two larger sources were limited to values below approximately 8600 sec by electrical breakdown.

Fig. 6 gives a comparison of the overall power efficiencies of the three engines over a range of specific impulse values. The curves for the two larger engines are parallel, indicating similar performance gains with increasing specific impulse. In the range of impulse values investigated the efficiency of the 5-cm source increased more rapidly with increasing impulse than that of the two larger sources, as might be expected in view of its initially poor performance. The performance of the sources increased with increasing size, but the difference between the 10- and 20-cm source engines was not felt to be significant.

Before drawing general conclusions on the relative merits of the three engines, several factors affecting the performance as presented must be considered. The 10-cm-diameter source was evolved from an electron-bombardment engine program at Lewis in which over 200 hr of operation had been performed with this size source. The 20- and 5-cm sources were scaled from the 10-cm source and operated in a manner found suitable for the 10-cm model. Approximately 6 hr of operation have been conducted on each of the large and small sources. It would not be unreasonable to assume that the 5- and 20-cm sources were at some disadvantage because of this difference in operating time.

The overall power efficiency of an ion rocket employing an electron-bombardment ion source is defined as the ratio of the beam power divided by the sum of the beam, magnet, filament, ion chamber, and accelerator impingement

powers. For a complete performance comparison, the effect of scaling on the various sources of loss should be considered.

Impingement power. - The accelerator impingement power is so small that it can be neglected. Also, it is shown in Fig. 3 to be directly proportional to engine size at the scaled magnetic field strength.

Magnet power. - For operation at scaled magnetic field strengths the ampere turns should be constant (coil diameter varies as engine diameter). Thus for the same size wire and the same current the loss and weight should both be proportional to diameter. But the beam power increases as accelerator area, or diameter squared. Hence a larger engine is seen to be more efficient for magnetic field power. The magnetic field coil on the 20-cm engine was closely wrapped about the source, as seen in Fig. 1, and represents a near optimum design. The coils used on the 5- and 10-cm sources had large diameter, adjustable windings and were not optimum.

Filament heating power. - For the same filament life the temperature should be about the same and the power loss should be proportional to the ion chamber emission current. Thus filament power should vary as ion chamber discharge power. None of the filaments used in the tests were optimized.

Ion chamber power. - As was seen in Fig. 2(c), the ion chamber performance of the 20-cm-diameter source was substantially the same as that of the 10-cm-diameter source, while the performance of the 5-cm-diameter source was much poorer. These experimental results agreed with the theoretical considerations of radial potential drop in the plasma.

Thus, in considering all the losses, there are definite problems in making smaller electron-bombardment engines without large reductions in overall power efficiency. In the other direction, there is no loss that should

increase an appreciable amount with increasing size, and the magnetic field loss should even decrease. The power efficiency of large electron-bombardment ion rockets should therefore at least equal that of the present size.

The very marked effects of ion chamber plasma density and ion beam current density have not been considered in the preceding discussion. Some insight into the effects of high current density operation might be gained by referring to the last equation for radial potential difference. The radial potential difference was found to be inversely proportional to the product of diameter and current density. Thus an increase in current density should have the same effect as an increase in size. To verify this conclusion experimentally, the 5-cm-diameter source was operated with an ion beam current of $1/8$ amp and a specific impulse of 6300 sec. The ion chamber loss (ion chamber discharge only) was 1200 electron-volts/beam ion. This ion chamber performance was much closer to that observed for the 10- and 20-cm-diameter sources. The improvement in ion chamber performance also showed up in improved overall power efficiency, which was 75 percent.

CONCLUDING REMARKS

Changing the size of an electron-bombardment ion chamber affects both the containment of high-velocity ionizing electrons and the radial potential drop in the plasma in the chamber. The containment is made similar if the product of magnetic field strength and chamber diameter is held constant, as was done during most of the comparison. The radial potential drop is more of a problem and tends to cause large losses in small chambers. What little data were obtained for varying density indicate that density changes should cause effects similar to size changes. That is, high density operation should decrease the radial potential drop.

The smallest engine gave inferior performance, but there was little change in going to an engine diameter larger than 10 cm. The effect of size on overall performance was substantially the same as on ion chamber performance. This result is to be expected since the ion chamber discharge and filament heating current are the two largest losses in most electron-bombardment ion rockets. The magnetic field loss, which is the only other large loss, should actually decrease relatively as the size increases.

The major interest for space propulsion will be for larger rather than smaller engines. As far as ion chamber performance is concerned, there appears to be no size limit on the electron-bombardment ion rocket. Practical engineering problems associated with large accelerator structures may be the ultimate limit, but no problems of this nature were encountered with the 20-cm-diameter source.

REFERENCES

1. Kaufman, Harold R.: An Ion Rocket with an Electron-Bombardment Ion Source.
NASA TN D-585, 1961.
2. Kaufman, Harold R., and Reader, Paul D.: Experimental Performance of Ion
Rockets Employing Electron-Bombardment Ion Sources. ARS Paper no. 1374-60,
1960.

FIGURE LEGENDS

(a) Photograph.

(b) Cutaway.

Fig. 1. - Concluded. 20-cm-diameter engine.

(a) 17-Gauss field.

(b) 32-Gauss field.

(c) Scaled field. Field strength \times Engine diameter = constant.

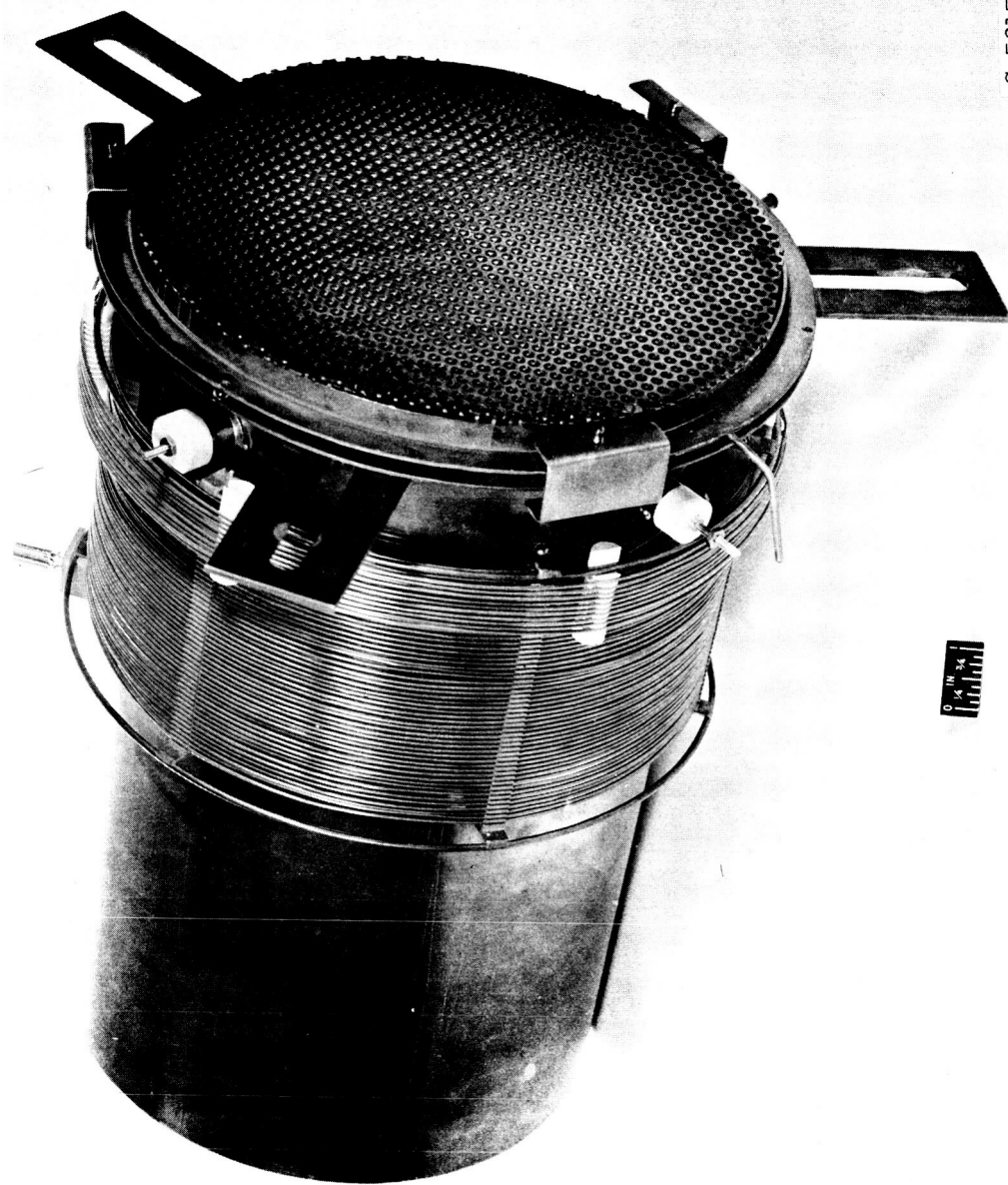
Fig. 2. - Ion chamber performance for varying ion chamber potential difference for constant and scaled magnetic field strengths.

Fig. 3. - Effect of magnetic field strength on accelerator impingement. Ion chamber potential difference, 50 v.

Fig. 4. - Effect of magnetic field strength on ion chamber performance with an ion chamber potential difference of 50 v.

Fig. 5. - Effect of accelerating potential on ion chamber performance.

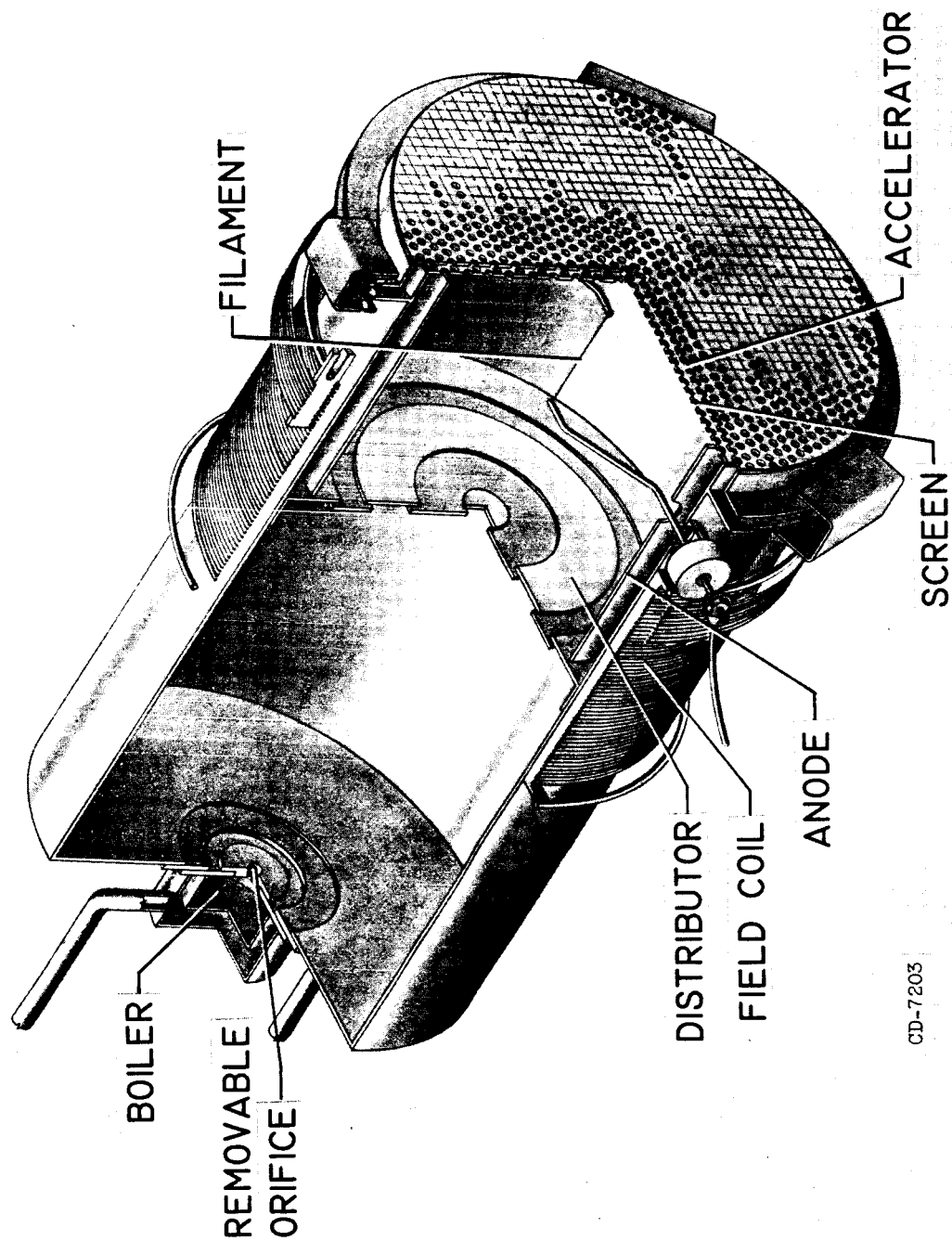
Fig. 6. - Effect of accelerating potential on overall power efficiency.



C-56157

(a) Photograph.

Figure 1. - 20-cm-diameter engine.



CD-7203

(b) Cutaway.

Figure 1. - Concluded. 20-cm-diameter engine.

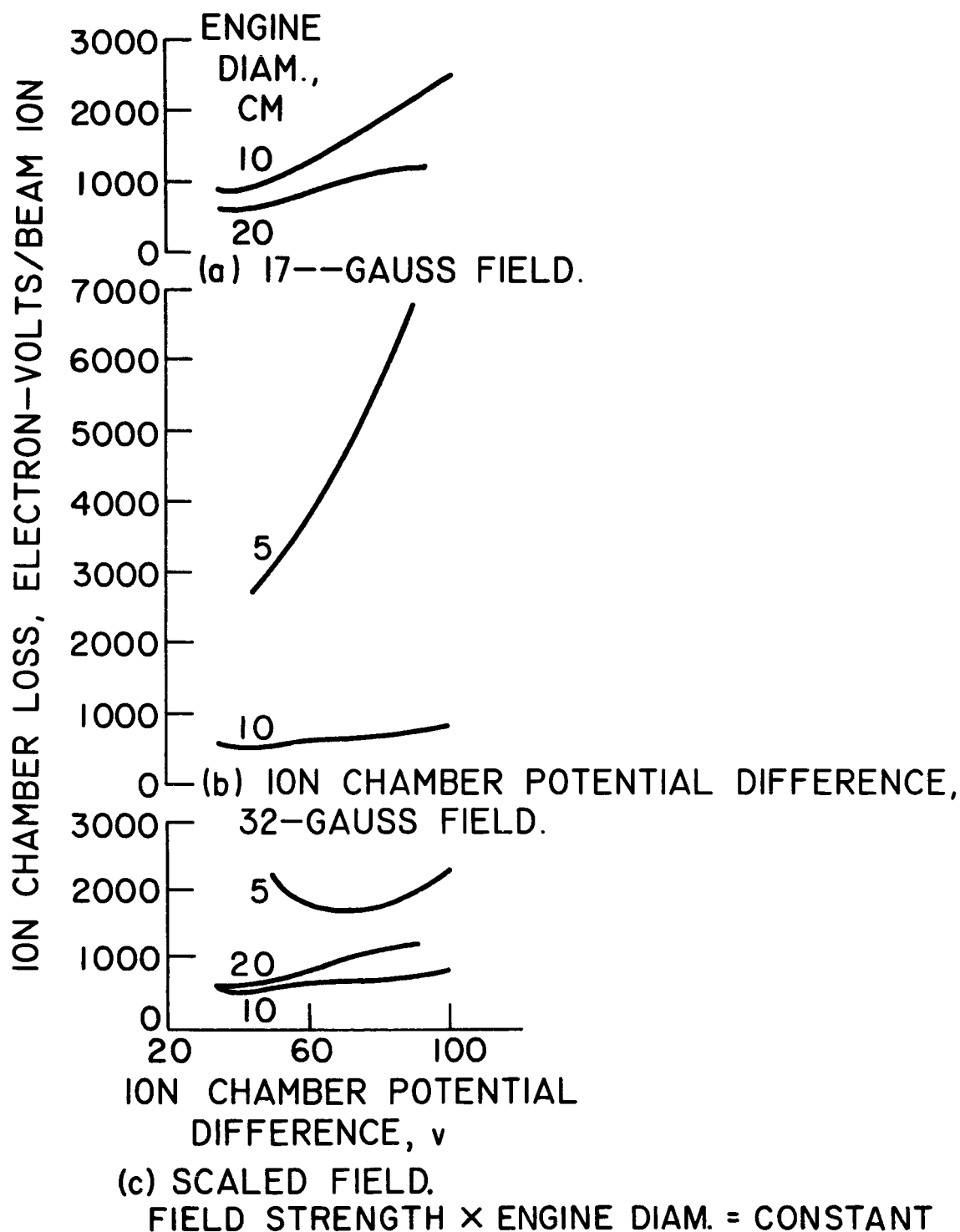


Figure 2. - Ion chamber performance for varying ion chamber potential difference for constant and scaled magnetic field strengths.

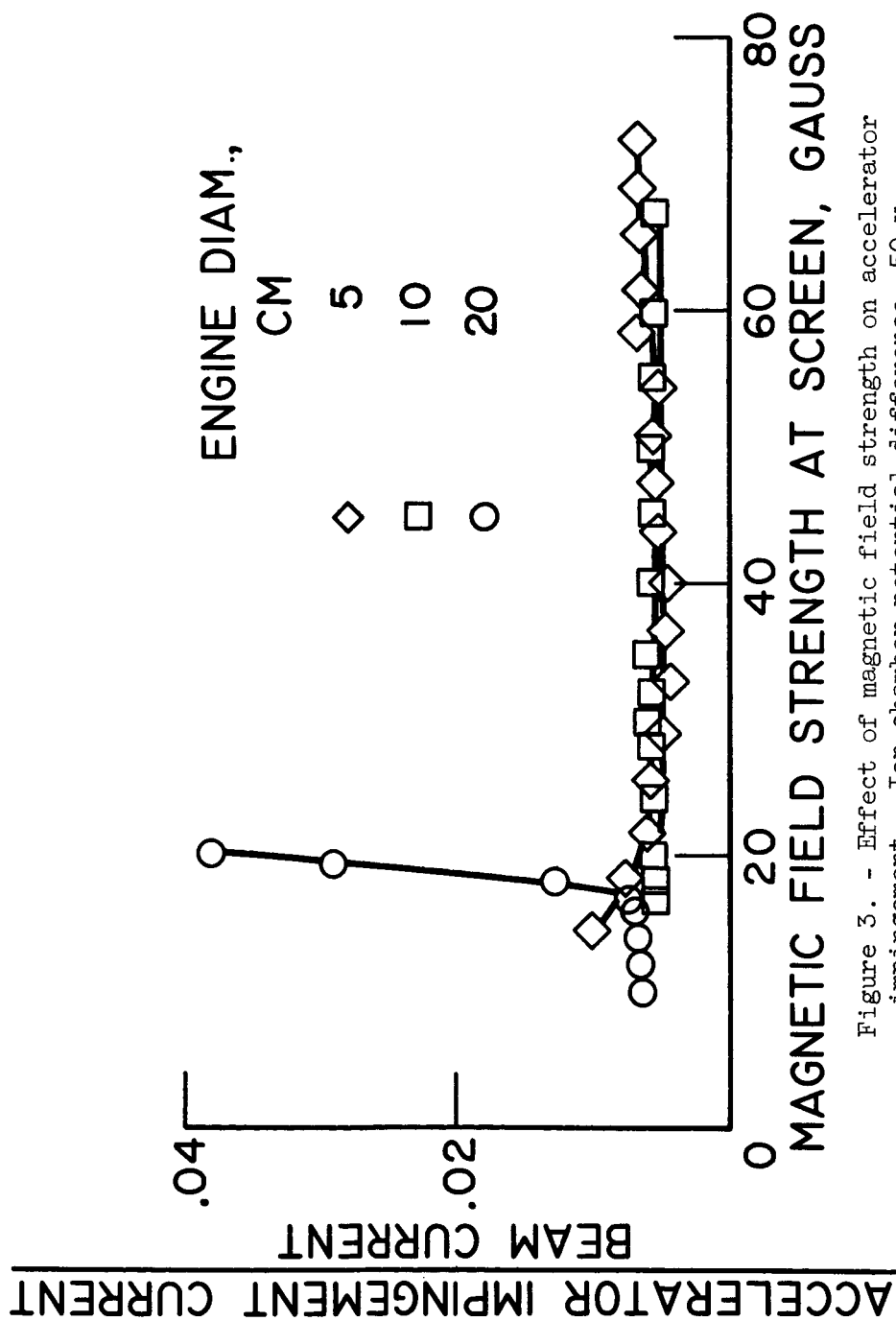


Figure 3. - Effect of magnetic field strength on accelerator impingement. Ion chamber potential difference, 50 v.

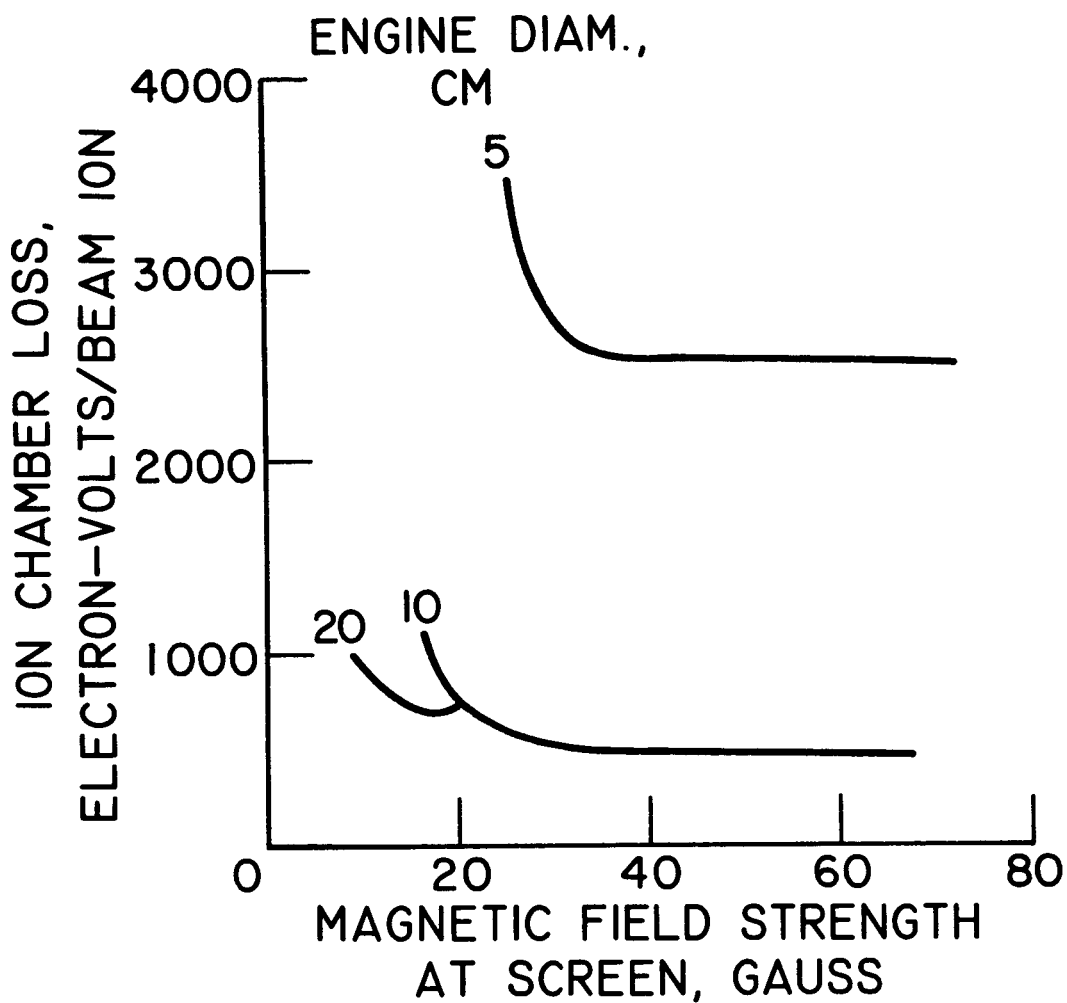


Figure 4. - Effect of magnetic field strength on ion chamber performance with an ion-chamber potential difference of 50 v.

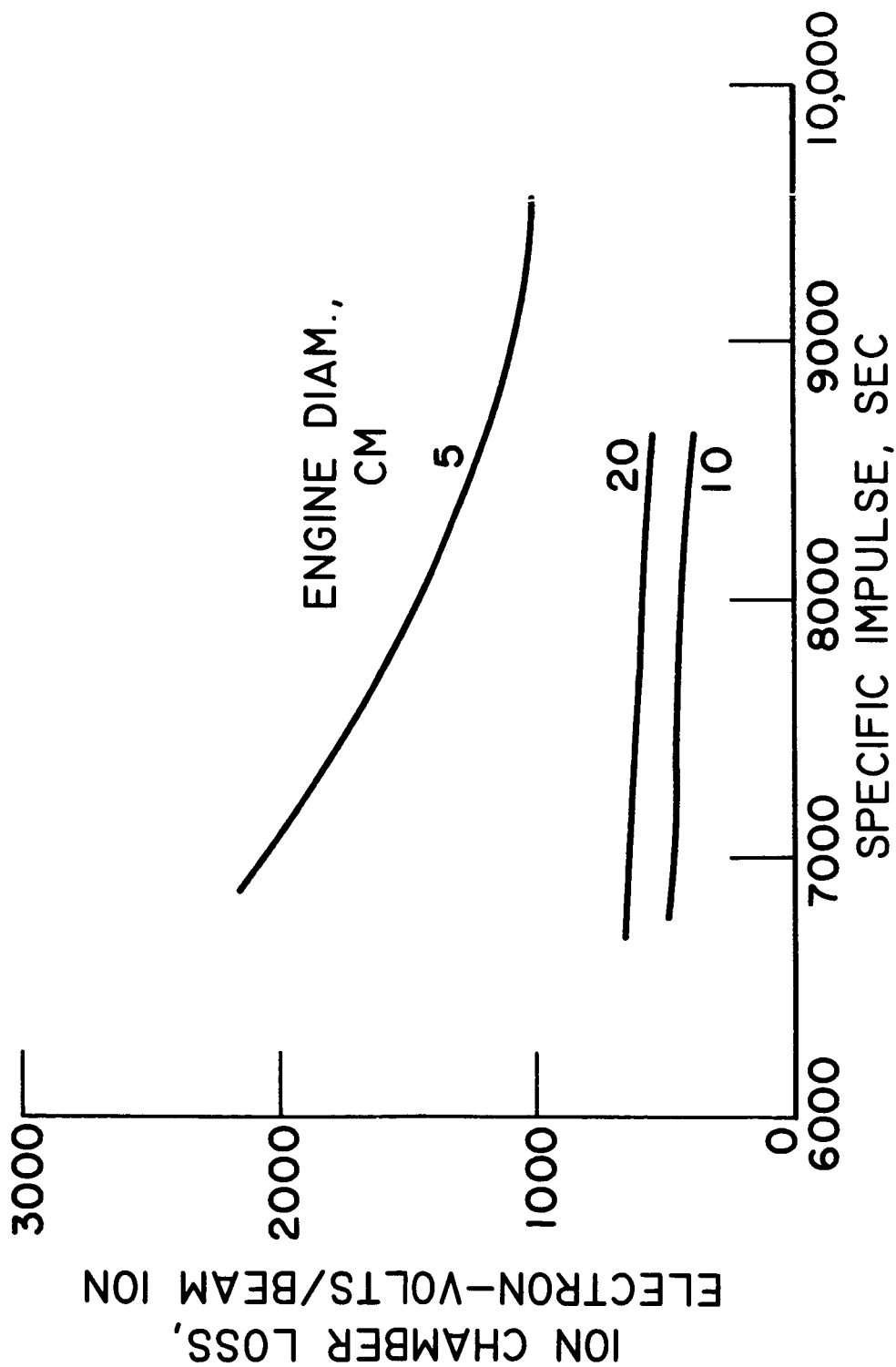


Figure 5. - Effect of accelerating potential on ion chamber performance.

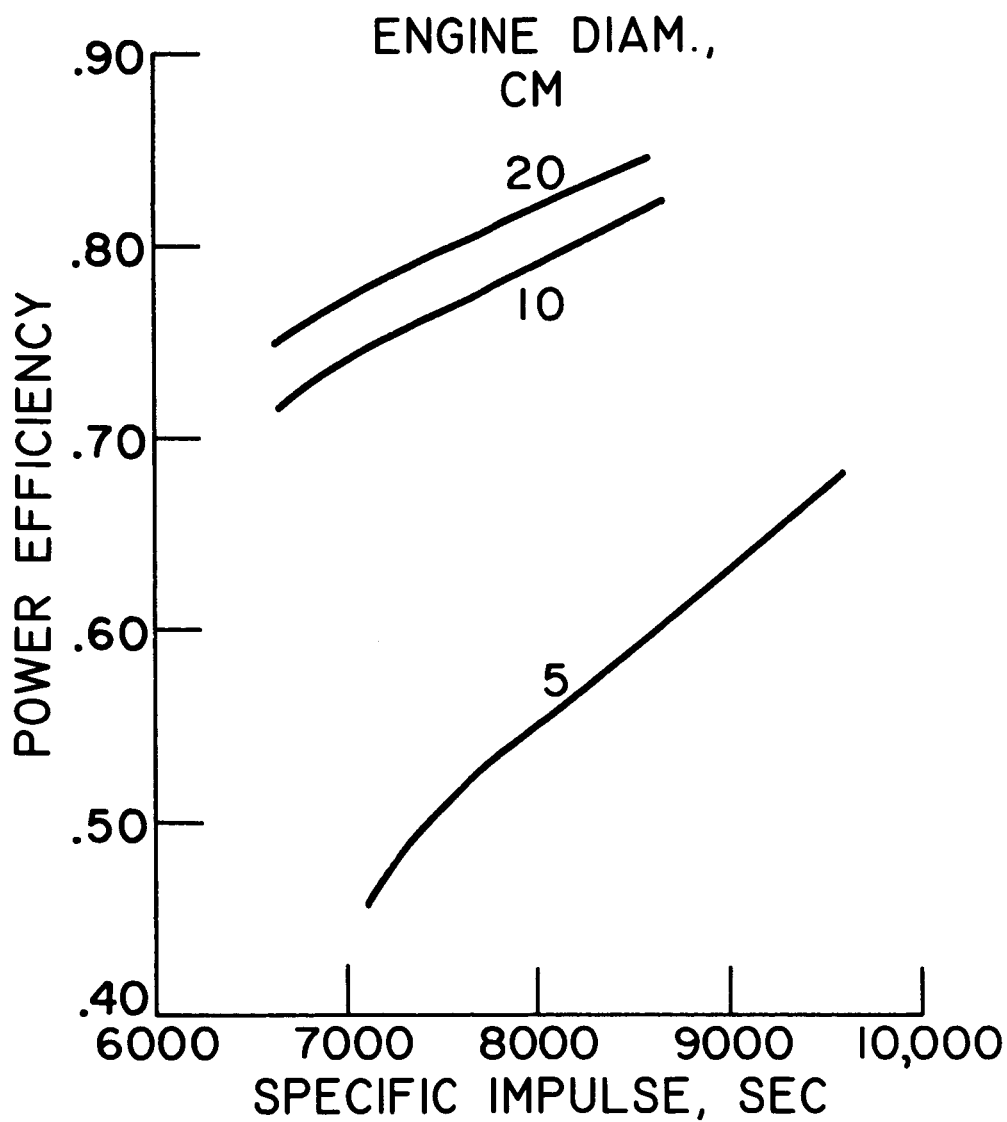


Figure 6. - Effect of accelerating potential on overall power efficiency.